Ground motion relations while TBM drilling in unconsolidated sediments

Michael Grund[1]*, Joachim R. R. Ritter[1], Manuel Gehrig[2]

[1] Karlsruhe Institute of Technology, Geophysical Institute

Hertzstr. 16, 76187 Karlsruhe, Germany

[2] Herrenknecht AG, Research & Development, Traffic Tunnelling

Schlehenweg 2, 77963 Schwanau-Allmannsweier, Germany

* corresponding author: michael.grund@kit.edu, Tel: +49 (0)721 608 44491,

Abstract

The induced ground motions due to the tunnel boring machine (TBM), which has been used for the drilling of the urban metro tunnel in Karlsruhe (SW Germany), has been studied using the continuous recordings of seven seismological monitoring stations. The drilling has been undertaken in unconsolidated sediments of the Rhine

river system, relatively close to the surface at 6-20 m depth and in the vicinity of many historic buildings. Compared to the reference values of DIN 4150-3 (1-80 Hz), no exceedance of the recommended peak ground velocity (PGV) limits (3-5 mm/s) was observed at the single recording site locations on building basements during the observation period between October 2014 and February 2015. Detailed analyses in the time and frequency domains helped with the detection of the sources of several specific shaking signals in the recorded time series and with the comparison of the aforementioned TBM induced signals. The amplitude analysis allowed for the determination of a PGV attenuation relation (quality factor $Q \sim 30\text{-}50$) and the comparison of the TBM-induced ground motion with other artificially induced and natural ground motions of similar amplitudes.

Keywords: TBM tunnelling, induced ground motions, unconsolidated sediments, PGV, attenuation relation, seismological analysis

1. Introduction

In the city center of Karlsruhe a metro tunnel was constructed with ~3 km length from the Durlacher Tor place in the east to the Mühlburger Tor place in the west (Fig. 1). Drilling is at 6-20 m depth from east to west mainly below the water table where the subsurface consists of unconsolidated sediments composed of gravel and sand. After the initial commissioning of the tunnel boring machine (TBM) called *Guilia* in November 2014, the final completion of the tunnel was done in September 2015. The tunnel tube measured 9.30 m in diameter and was drilled while the tram and railway traffic continued at the surface. Drilling inside a city and directly along buildings and

infrastructure must be done with special care to avoid structural damage or even disturbances to neighboring inhabitants (e.g. Ocak 2009). Monitoring of TBM-induced ground motions is mandatory in such situations (e.g. Greenfield 1983; Flanagan 1993; Carnevale et al. 2000; Ho and Wong 2010; Benslimane et al. 2010). Predictions for expected peak ground velocity (PGV) based on drilling and lithological subsurface parameters have also been undertaken (Speakman and Lyons 2009) to estimate drilling-induced ground motions before actual operation of a TBM. In Germany, the technical rules in DIN 4150-3 (1999) define reference values for temporary as well as continuous ground motions. According to these values PGV=3-5 mm/s should not be exceeded at historic and residential buildings at 1-10 Hz frequency (or 3-15 mm/s at 10-50 Hz and 8-20 mm/s at 50-100 Hz) to avoid possible damage. Where social disturbance is required to be monitored to local inhabitants, the ground motion should be approximately one order of magnitude less (DIN 4150-2 1999).

2. Seismic recording network

The tunnel construction started directly in front of the campus of the Karlsruhe Institute of Technology (KIT) and was as close as a few meters from its historic buildings, some dating back to the founding period of Karlsruhe in the 18th century. In order to review the possible effects of such near-building drilling, continuous measurements of the ground motions along this part of the TBM route with seismological stations of the KArlsruhe BroadBand Array (KABBA) were undertaken. Six sites (CST01, 02, 03, 04, 06 and 07) were placed in cellars of KIT buildings (Fig. 1). One recording station (CST05, accelerometer type Hyposensor) was installed into a mini-borehole at 60 cm depth as free-field station close to CST02 on the KIT campus (see Fig. 2). During the tunnel drilling, on 11/12/2014 stations CST01 and

CST04 were removed and reinstalled as CST06 and CST07 towards west along the drilling route (see Fig. 1). Three-component (vertical, N-S and E-W) velocity-proportional sensors of type Lennartz 5s (LE-3D/5s) were used at CST01, CST02, CST03, CST06 and CST07. In addition an accelerometer of type Episensor recorded at CST04 just beside CST01. Earthdata PR6-24 recorders with 24-bit digitizers and GPS time synchronization were used for data acquisition and storage. The data sampling rate was set at 200 Hz at each recording site.

3. Preprocessing of recorded seismic data

The recorded seismic data was uniformly preprocessed to allow a direct comparison of the results with the different sensors. Firstly, means and linear trends were removed from all time series. The influences of the different response functions of the sensors were then removed (deconvolution) to finally get instrument independent time series of the true ground motion (velocity) which are directly comparable in amplitude and phase. Since the recordings of the Episensor and Hyposensor are in units of mm/s^2, the corresponding time series were integrated to velocity proportional ground motions in m/s as required by DIN 4150. The resulting time series were filtered forward and reverse with a second-order Butterworth bandpass filter with different corner frequencies (see following sections). Since for a sampling rate of 200 Hz the recorded signals below 100 Hz are already influenced by the flank of the anti-alias filter during the data acquisition, the highest studied corner frequency was 80 Hz.

4. Identification and assignment of recorded seismic signals

An example of a time window consisting of seven days with continuously recorded ground motion (bandpass filtered 1-80 Hz) is presented in Fig. 3. The top panel

shows the recorded time series of the vertical component (Z) of station CST01 in mm/s while the bottom panel displays the corresponding frequency content over time in a so called spectrogram. Distinctly, for both ranges, the day vs. night differences over the whole week are clearly visible with man-made high-amplitude noise during daytime and less noise during nighttime. With the start of the TBM operation on 17/11/2014 (TBM start), dominant broad frequency signals at about 1-30 Hz are induced which are visible as vertical reddish stripes in the frequency domain. The operation start (first two vertical red stripes) is also visible in the time domain (see A and B in Fig. 3), since the amplitude values exceed the permanent background noise level for a short time period during the drilling process. Furthermore, Fig. 3 demonstrates that other signals, recorded before the TBM operation start, also exceed the continuous background noise in the same way as the signals generated by the TBM. Most of these high amplitude signals are caused by passing trains and trams above the tunnelling path. Signals generated due to the rotation of the cutting wheel of the TBM at around 2.5 cycles per minute (0.04 Hz) can not be resolved in the recorded ground motions, since the sensitivity of the used sensors is too low, given an eigenperiod of 5 s (0.2 Hz, LE-3D/5s).

Besides these mostly temporary noise signals with varying frequency content, monofrequent signals are also detectable, e.g. at 50 Hz which correspond to the frequency of the electric power supply. Fractions of the 50 Hz are also clearly visible and these belong to electrical motors with 25 Hz and 12.5 Hz. The 16.7 Hz signal was identified as the dominant frequency of the separation plant for the excavated soil and sediment which is located around 150 m east of the start location for drilling on the Durlacher Tor place (Fig. 1). The timestamps of the tunnelling protocol show that the separation plant starts several minutes before drilling continues and ends a

few minutes after the actual drilling operation. For the identification of signals from the separation plant, we recorded its ground motions over a short time period before and during operation directly on its base with one of the LE-3D/5s sensors (Fig. 4). Before the separation plant started operation, besides the mentioned frequencies of 50 Hz and 25 Hz, only two dominant monofrequent signals at 30 Hz and 60 Hz were observed on all three components in the frequency range (Fig. 4b, d and f). After powering up, componentwise several frequency bands are induced with dominant signals at 16.7 Hz and 65 Hz. Furthermore, on the vertical and E-W component a signal at around 55 Hz was detected. Since the largest amplitudes with up to 0.8 mm/s are recorded on the vertical component (Fig. 4a), it can be inferred that the main vibration energy of the separation plant is generated due to rotating cyclones and shaking screens and is released in vertical direction. However, the signal at 16.7 Hz only occurred within the mentioned time periods and thus the separation plant could be identified as the only source, although generally the traction current in Germany also has a frequency of 16.7 Hz.

A comparison of the signals generated on 17/11/2014 (start of TBM operation) is shown in Fig. 5 for the two recording stations CST01 and CST03 at 06:00-12:00 (UTC). In addition to an increase of the signal amplitudes due the TBM operation observable in the time domain, the induced signals in the frequency domain are also clearly visible at some distance (CST03 ~130 m to drilling start point, see Fig. 1). As expected the amplitudes of the signals induced by the separation plant decrease with increasing distance.

The standard drilling operation is characterized by two repeating processes. First the actual excavation of the underground is done with the cutter head. Then, when about 2 m of advancement is achieved, which takes about 30 minutes under normal

conditions for the tunnel in Karlsruhe, the cutter head is stopped and the concrete segments are fixed to the walls, which takes about 20-30 minutes. Two cutting operations with increased signal amplitudes are displayed in Fig. 5.

A more detailed view on the differences between TBM signals and train or tram induced ground motions (1-80 Hz) is presented in Fig. 6a for the vertical component of recording station CST07. Two passing trams induce a frequency band of about 1-80 Hz and about 15 s duration. Before the TBM continues to move on (dashed black line) frequencies of 1-80 Hz are induced which are mainly caused by powering up different engines and machines needed for the drilling process like compressors etc. During this powering up phase the highest ground motion amplitudes (-20 dB, red) are in the frequency range 5-25 Hz, higher frequencies up to 80 Hz have relatively lower amplitudes (-40 dB, yellow). With the beginning of the new drilling cycle higher amplitudes are induced (top panel) in this frequency range (about -20 dB up to 80 Hz), whereas the main energy is released at 1-15 Hz (0 to -10 dB, dark red, bottom panel). Therefore, almost no separation of signals induced by passing trams and the TBM is possible in the frequency domain during TBM drilling. Because station CST07 was sited around 475 m from the separation plant (Fig. 1), no dominant signal induced by the plant is detectable, neither in the time domain nor the frequency domain.

Besides the artificial ground motions, the phases of natural tectonic earthquakes are also detectable and can be compared to the induced ground motion. Fig. 6b shows signals of several passing trams as well as the *P*- and *S*-wave arrivals of an earthquake with magnitude M_L=3.4 close to Albstadt, Germany, about 100 km towards SE from Karlsruhe (LGB-RLP 2015). This was a typical earthquake with low frequencies (0.6-20 Hz) being observed at station CST07. Furthermore, the

waveform of the earthquake shows a distinct onset compared to the continuously increasing and decreasing amplitudes of the passing trams. Compared to the commonly induced frequency bands of trams and the TBM, for earthquakes an obvious differentiation in the frequency range is possible. Concerning the ground motion amplitudes, the tram and TBM induced signals are similar to earthquake waves of an event with magnitude 3-3.5 at 100 km distance from the source with such motions generally being hardly felt by residents at this distance.

The identification of passing trams within the recorded data (except periods when the TBM was active) is quite simple by observing the overlayed signals within identical time durations of at least two or three recording stations. Using stations CST01 to CST03, the first increasing signal amplitudes within box 1 in Fig. 7a are assigned to station CST01 (red signal, most eastern station, see Fig. 1), followed by an increase at CST02 (blue, middle station) and CST03 (green, most western station). For boxes 2 and 3, the same characteristics are observed which implies that these trams were moving from east to west and passing the stations in this order. The signals in box 4 display an inverse time sequence of increasing amplitudes and thus the corresponding tram was moving from west to east.

Considering the onsets of increasing amplitudes at different stations additionally allows us to estimate the velocities of different vehicles. Fig. 7b shows the signals simultaneously recorded at stations CST02, 03 and 07 versus the distance relative to CST02. For the first signal, onsets are marked with a red line and the corresponding slope results in an apparent velocity of around 55 km/h which is a typical velocity for a tram at this track section. As seen in Fig. 7a, since the first arrival order is CST02, 03 and 07, this tram was moving from east to west. The corresponding slope of the second line marking the onsets of decreasing amplitudes is lower, which results in a

velocity of around 20 km/h. This velocity is typical for a supply railway (rolling stock) which transports the cement segments and other material along the finished part of the tunnel to the TBM. From a location inspection during that time period (08:20 at 22/01/2015, UTC), we know that a fully loaded supply train was passing from east to west which coincides with the observed increasing signal amplitude order from recording station CST02 at first to CST07 at last.

5. Characteristics of TBM generated waves

To analyze the ground motion during the TBM operation over time, a sliding window procedure was applied. Using one hour long time windows of data (1-80 Hz) the rms (root mean square) amplitude was calculated to retrieve the average ground motion conditions in this time period. By plotting the selected rms amplitudes for each hour at one recording station against time, temporal changes in the ground motion recordings become visible.

Fig. 8 displays the rms amplitudes of the different recording stations while these were active. Up to the 99.73 % occurrence interval (rms calculated out of the measured amplitude values which lie within an interval of three standard deviations from zero, see e.g. Groos and Ritter 2009) the day/night change is visible (Fig. 8b) which is not observable in the interval containing rms values calculated out of all amplitude values (Fig. 8c). In the 68 % occurrence interval (one standard deviation away from zero) the advance of the TBM operation from east to west is clearly observable besides the day/night change (Fig. 8a). The rms values first increase up to a maximum rms value when the TBM reaches the recording station. Afterwards, the signal amplitudes decrease when the TBM moves away until the amplitudes are covered again by the background noise. Since stations CST01 and CST04 are located around 30 m east

of the drilling start point, no similar characteristics of increasing and decreasing rms values are observable for both stations in Fig. 8. By means of the amplitude values, it is also possible to see that station CST06 was located at a greater distance from the drilling route since the corresponding rms values in general are lower compared to the station sites closer to the drilling route (Fig. 1). Furthermore, longer downtime periods of the TBM are visible, e.g. during the Christmas break between 23/12/2014 and 07/01/2015 at the Kronenplatz (see Fig. 1). High rms values at station CST02 (> 99.73 % interval) probably result from addition signals of the train lines, possibly due to irregularities of the rails. The breakthrough of the TBM at the first slotted wall at Durlacher Tor is observable as an amplitude peak on 17/11/2014 (TBM operation start) at all simultaneously recording stations.

The maximum rms amplitudes are observed at recording station CST05 since the location in the mini-borehole close to the surface recorded surface waves as well as the occurrence of amplitude amplification due to the shallowest sediments. In contrast, the other sensors were placed on stiffer concrete floors.

The particle motion of the emitted seismic signals (bandpass filtered 1-35 Hz) is displayed in Fig. 9. The TBM was rotating just 10-20 m south of station CST03 (backazimuth (BAZ) about 0°) and about 70 m from station CST02 (BAZ ~ 80°). Due to the larger distance, the amplitudes are smaller by a factor of 2.5 at CST03 relative to CST02 (note the different scales of the corresponding particle motion diagrams). The ground motion is not polarized in a uniform way. This is interpreted as occurrence of a mixture and interference of different body wave types (compressional (P), and horizontally (SH) as well as vertically (SV) shear waves) which are excited by the rotating cutter head with its single cutting bits. Depending on the angle and direction of the motion of the cutting bits, either P, SH or SV waves are recorded at a

seismic station. We can neither identity clear vertically polarized Rayleigh waves nor horizontally polarized Love waves. Thus, we infer that surface waves do not play a major role in our recordings. This assumption is supported by the geometry of the source-receiver setting which is mainly a deep source (relative to the horizontal offset) for station CST03. Recordings from sources acting directly at the surface show a different behaviour, e.g. signals emitted by trucks hitting potholes at the surface are characterized by vertically polarized Rayleigh waves (Ritter and Sudhaus 2007).

To analyse the amplitude-distance relation during TBM operations for our area, the rms amplitudes (PGV) of selected time periods were computed at different stations (Fig. 10). The corresponding distances from the sensors to the operating TBM were estimated by considering the varying horizontal distances and an average drilling depth of 6 m. The spectrograms in Figs. 3, 5 and 6 reveal that the TBM mainly induced signals in a frequency band up to 30 Hz. Thus, all data was filtered between 1-30 Hz. Since during daytime the TBM signals are contaminated with induced signals with higher amplitude peaks of trams, cars and other traffic, the time windows to calculate the rms values are selected manually, mostly during night time operation. This selection reduces the influence of other noise sources and it ensures that the amplitude-distance analysis is not biased by artefacts not generated by the TBM.

Following Speakman and Lyons (2009), the PGV in mm/s generated by a TBM within the dominant frequency band at a given distance can be expressed as

$$\mathrm{PGV} = \frac{K}{d} e^{-\alpha d} \qquad (1)$$

where the values α (attenuation factor) and K are site and machine specific parameters and d is the distance from the source (TBM) in m. Geometrical spreading

for body waves is considered by the 1/d term. Measuring the PGV values generated by the TBM at different distances from one recording site allows us to estimate the site and machine specific parameters by

$$\alpha = \frac{-\ln(\frac{v_2 d_2}{v_1 d_1})}{(d_2 - d_1)} \qquad (2)$$

and

$$K = \frac{v_1 d_1}{e^{-\alpha d_1}} \qquad (3)$$

with v_1 and v_2 as measured PGV at distances d_1 and d_2.

Using equation (1) to fit our observed rms values leads to the fitting curves presented in Fig. 10 for the vertical components of stations CST02, 03, 05 and 06. Since the varying drill velocities in the beginning of the tunnel construction (dark blue colors in Fig. 10) would bias the data fitting, the corresponding PGV values were excluded before the determination of the parameters α and K. Furthermore, it should be noted that for very close distances to the sensors the TBM shield with its large diameter violates the assumption of a point source (Flanagan 1993). At a distance of about 250 m, the rms values of signals generated by the TBM reach the level of the background noise and thus no signal identification is possible anymore.

In seismological context, the amplitude decay as result of damping is represented by the so called quality factor Q which describes anelastic or scattering attenuation or both coincidentally. Q is inversely proportional to attenuation and thus low Q values indicate high damping. In the following, the latter case is dealt with which is called effective attenuation. Following Badri and Mooney (1987), Q can be expressed as:

$$Q = \frac{\omega}{2\alpha v} \qquad (4)$$

with ω as angular frequency $\omega = 2\pi f$ and v as seismic velocity for a specific medium. By using v = 1500 m/s as a typical compressional wave velocity for unconsolidated sediments (Studer et al. 2008) and f = 30 Hz, the corresponding Q factors for our determined α values are presented in Fig. 10. For stations CST02, 03 and 06 in cellars the determined Q factors are in an order of 30 to 50, whereas the Q factor for the mini-borehole station CST05 is around 70. The lower damping at CST05 may be due to a better coupling of the buried borehole sensor with the ground as well as amplitude amplification effects due to near-surface soil layers. The range of the Q values clearly indicates that wave propagation in loose and partially unconsolidated material (typical $Q \sim$ 5-100) takes place, whereas higher Q values are expected for solid rock ($Q > 100$) (Schön 2011). The determined Q values of 30-50 are compatible to rock material like clay and marl (Lavergne 1986; Stevenson et al. 2002), water-saturated sandstone (Schön 2011) or water saturated sand and gravel deposits (Stevenson et al. 2002; Campbell 2009) as measured in other experiments. Thus the Q values derived from Fig. 10 can be well explained with the partly water-saturated gravels and sands which are excavated by the TBM and which belong to the sedimentary deposits of the Rhine river.

6. Estimation of peak ground velocities (PGV) following DIN 4150

The PGV analysis was done separately for each single recording station and component. During the time periods given in Fig. 11 the absolute PGV values were estimated for each recording station in hour-long time windows for all three components. To minimize artifacts due to filtering, an additional 10 minutes of data

were added at the beginning and the end of each hour-long time window and a taper was applied. The single time series initially were filtered with a second order Butterworth bandpass filter forward and reverse with corner frequencies of 1 Hz and 80 Hz to determine the PGV values (TBM, trams, traffic) according to the frequency bands recommended in DIN 4150-3 (1999) for short-term vibrations as well as continuous shaking. Time windows during station maintenance works were removed from the analysis to avoid artifacts. Finally, the absolute maximum PGV value during all time windows of all three components represents the maximum ground motion at the corresponding recording station. Fig. 11 shows these PGV values for the single stations and Table 1 lists the PGV values. For stations CST01-04 and CST07 in basements the measured PGV values reach 0.5-0.65 mm/s (see Table 1 for precise values of all components). The lower value of 0.39 mm/s at station CST06 (Fig. 11) in another cellar can be explained by the larger distance of around 20 m to the drilling route. As discussed above, the comparatively high PGV values at the free-field borehole station CST05 mainly result from the large amplitudes of surface waves as well as amplification effects due to the soft soil close to the surface. The measured maximum amplitude overall in our investigation period (2.08 mm/s at CST05) was generated by a passing train. Considering the reference values of DIN 4150-3(1999) with 3 mm/s for landmarked historic buildings and 5 mm/s for standard structures no exceedance of permitted PGV values (3 mm/s) in the frequency band 1-80 Hz was observed during the investigation period October 2014 and February 2015, although the TBM passed all monitored buildings in this time span. As seen in the previous sections, in general, primarily temporary ground motions induced by large trams exceed the signals generated by the TBM. It should be noted that in higher floors the PGV can be much larger than on the basement level, however our aforementioned measurements do not indicate that critical values should be expected. Compared to

PGV values reported by Flanagan (1993) for TBM tunnelling in hard rock (5.5 mm/s at 5 m distance, 2.2 mm/s at 10 m and 0.6 mm/s at 25 m) our PGV values are significantly lower. A reason for this could be the low Q values in the unconsolidated fluvial sediments in Karlsruhe compared to higher Q values in hard rock.

7. Summary and conclusions

During TBM drilling for an urban metro tunnel, the ground motions in Karlsruhe were studied between October 2014 and February 2015 with seven seismological sensors. Compared to other studies in hard rock (Flanagan 1993; Fornaro et al. 1993; Carnevale et al. 2000) the frequency content induced by the TBM with maxima between 5 Hz and 80 Hz is similar, although the Karlsruhe metro tunnel was drilled in unconsolidated fluvial sediments close to the surface. The most specific ground motion signals related to the TBM operation are best detectable in the frequency domain since the low amplitudes are masked due to the high background noise. Furthermore, other man-made generated signals like passing trams and trains show similar broadband frequency contents up to 80 Hz (Fig. 6). Some monofrequent signals were assigned to the power supply (50 Hz) and the separation plant for the excavated soil and sediment (16.7 Hz).

In Karlsruhe, recorded ground motion amplitudes of an earthquake with magnitude M_L=3.4 at around 100 km epicentral distance are in the same order of signal amplitudes generated by trams and trains in the near surrounding of the recording stations (Fig. 6b). Moreover, at most recording stations, the recorded signals generated by passing trams have higher amplitude values than the ground motions induced by the TBM. Considering determined rms values of 60 minute time windows for each station, the highest ground motion rms-amplitudes were measured at the

shortest distance between source and sensor when the TBM passed the corresponding station (Fig. 8). These observations imply that the TBM operation will disturb nearby residents no more than passing trams in general. Additionally, the PGV values measured at the single stations between November 2014 and February 2015 are far below the corresponding reference values of DIN 4150-3 (1999) and thus no damage on buildings is expected (Fig. 11). Only one station (CST05, free-field) shows slightly increased ground motion amplitudes (PGV ~ 2 mm/s) compared to the other stations (sited in cellars, some in historical buildings) which mainly is caused by the location close to the surface. However, no exceedance of the reference values of 3 mm/s for historical buildings or 5 mm/s for standard buildings (DIN 4150-3 1999) was observed during the investigation period at any recording station (Table 1). Nevertheless, due to structural properties of buildings, the amplitudes recorded in higher floors can be larger than on the basement level.

The analysis of the relation between distance and ground motion amplitudes induced by the TBM reveals typical decay characteristics which can be explained by an exponential function and station specific parameters including a damping term (Fig. 10). This leads to the low Q values of 30-50. A comparison of the rms amplitude values observed for different distances between source (TBM) and recording station in this study with rms values determined by Ho et al. (2010) shows similar orders, although no specific medium is indicated for which their given rms values were estimated. At a distance of about 250 m the signals generated by the TBM in Karlsruhe are not detectable anymore, since these are covered in the background noise.

The ground motion relations analyzed in this study reveal that the amplitudes of signals induced by mankind (e.g. TBM, trams or separation plant) can have a similar

order to arriving waves of a natural earthquake (M_L=3.4, around 100 km epicentral distance) which in general are not felt by any residents. In contrast, the amplitudes of ground motions generated by the daily railway traffic in most cases are higher than the signals induced by the TBM. This comparison may help to reduce concerns that TBM drilling within an urban area could lead to damage and disturbance to infrastructure and humans. Ultimately, the ground motion characteristics highly depend on the properties of the subsurface (hard rock, sediments) and the type of TBM and shaking can vary intensely due to geological conditions.

Acknowledgements

References

Badri M, Mooney HM (1987) Q measurements from compressional seismic waves in unconsolidated sediments. Geophysics 52(6):772-784

Benslimane A, Anderson DA, Munfakh N, Zlatanic S (2005) Ground borne vibration on the East Side Access Project Manhattan segment: issues and impacts. In: Erdem Y, Solak T (eds)

Underground Space Use: Analysis of the Past and Lessons for the Future, Vol. 1. Taylor & Francis, Boca Raton pp 449-454

Campbell KW (2009) Estimates of shear-wave Q and κ_0 for unconsolidated and semiconsolidated sediments in Eastern North America. Bull Seism Soc Am 99(4):2365-2392

Carnevale M, Young G, Hager J (2000) Monitoring of TBM-induced ground vibrations. In: Ozdemir (ed) North American Tunneling ' 00. Balkema, Rotterdam, pp 374-384

DIN 4150-2 (1999) DIN 4150-2:1999-06, Erschütterungen im Bauwesen - Teil 2: Einwirkungen auf Menschen in Gebäuden. Deutsches Institut für Normung e.V., Berlin

DIN 4150-3 (1999) DIN 4150-3:1999-03, Erschütterungen im Bauwesen - Teil 3: Einwirkungen auf bauliche Anlagen. Deutsches Institut für Normung e.V., Berlin

Flanagan RF (1993) Ground vibration from TBMs and shields. Tunnels and Tunnelling 25(10):30-33

Fornaro M, Patrucco M, Sambuelli L (1993) Vibrations from explosives, high energy hydraulic hammers and TBMs; experience from Italian tunnels. In: Burger H (ed) Options for Tunnelling. Elsevier, Amsterdam, pp 829-838

Greenfield RJ (1983) Seismic analysis of tunnel boring machine signals at Kerckhoff Tunnel. United States Army Corps of Engineers, miscellaneous paper GL-83-19

Groos JC, Ritter JRR (2009) Time domain classification and quantification of seismic noise in an urban environment. Geophys J Int 179:1213-1231

Ho W, Wong B, Raine A, Kwok K (2010) Groundborne noise and vibration impact from rock tunnel boring machines. Wilson Acoustics Limited. http://www.wal.hk/downloads/Goundborne_Noise_&_Vibration_Impact_WAL.pdf. Accessed: 11 August 2015

Ho W, Wong B (2010) TBM Groundborne Noise Prediction Models. Tunnelling Journal April/May: 28-32

LGB-RLP (2015) Erdbebenereignisse lokal. http://www.lgb-rlp.de/ler_action.Datum.25651.html. Accessed: 20 July 2015

Lavergne M (1986) Seismic Methods. Editions Technip, Paris

Ocak I (2009) Environmental effects of tunnel excavation in soft and shallow ground with EPBM: the case of Istanbul. Environ Earth Sci 59:347-352

Ritter JRR, Sudhaus H (2007) Characterization of small local noise sources with array seismology. Near Surface Geophys 5:253-261

Schön J (2011) Physical properties of rocks - a workbook. Handbook of petroleum exploration and production, Vol. 8. Elsevier, Amsterdam

Speakman C, Lyons S (2009) Tunnelling induced ground-borne noise modelling. In: Zander AC, Howard CQ (eds) Acoustics 2009: Research to Consulting, Proceedings of the annual conference of the Australian Acoustical Society. pp 1-5

Stevenson IR, McCann C, Runciman PB (2002) An attenuation-based sediment classification technique using Chirp sub-bottom profiler data and laboratory acoustic analysis. Marine Geophys Res 23:227-298

Studer JA, Laue J, Koller M (2008) Bodendynamik: Grundlagen, Kennziffern, Probleme und Lösungsansätze. Springer, Berlin & Heidelberg
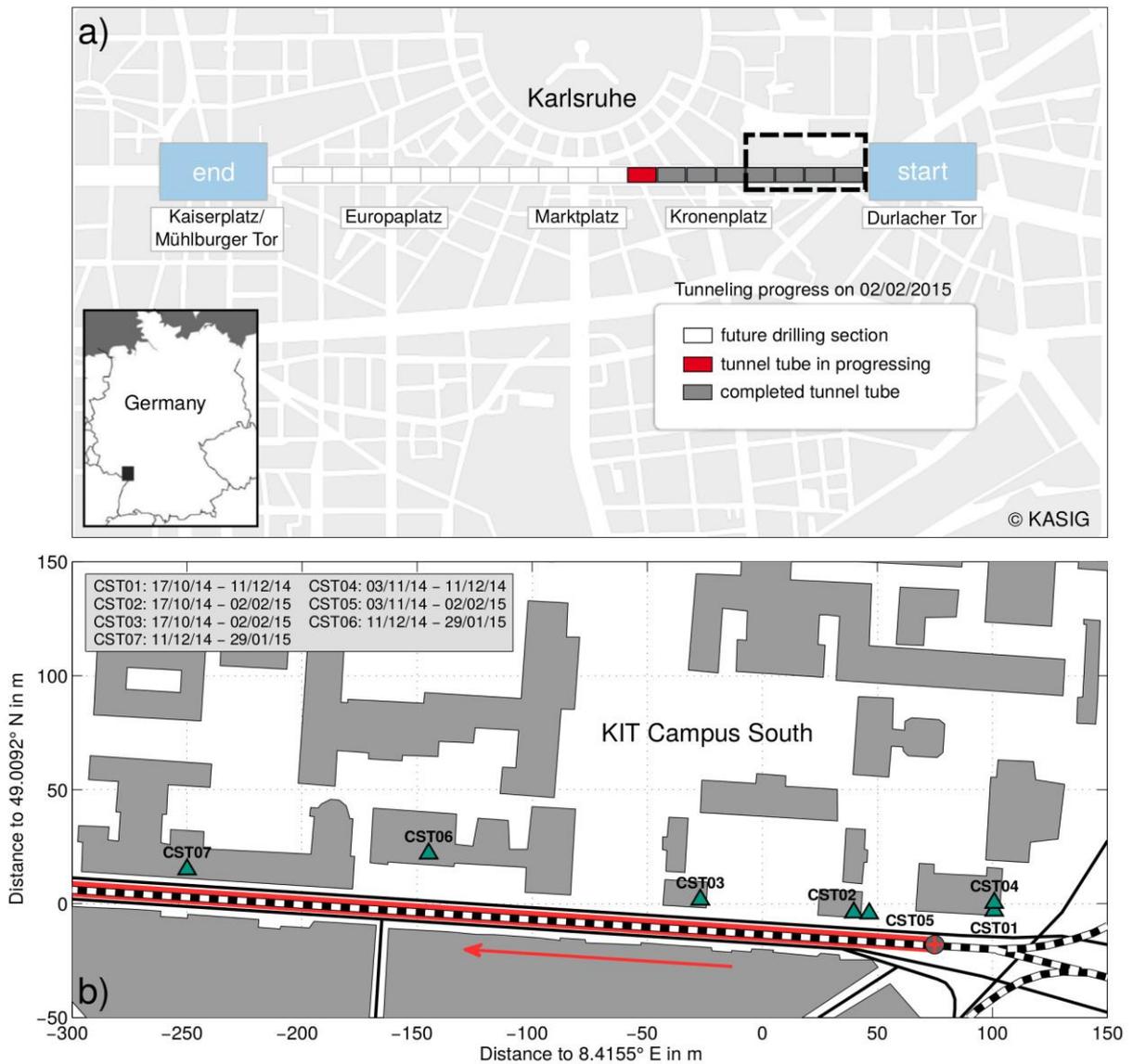
Fig. 1 a) View of downtown Karlsruhe with the whole tunnel drilling route (start to end). Modified with kind permission of KASIG - Karlsruher Schieneninfrastruktur-Gesellschaft mbH. © KASIG. The inset map indicates the location of Karlsruhe within Germany. b) Detailed view of the investigation area marked as dashed black box in a) with the installed seismic stations CST01-07 (recording periods in gray box in upper left corner) as well as the route and direction of the tunnel drilling (red line and arrow) and the starting point (red cross). Gray areas indicate buildings and black lines roads. Rails for trams are marked as dashed lines (black and white)

Fig. 2 Seismological sensors used for our analysis. Left: LE-3D/5s and Episensor at station sites CST01 and CST04. The LE-3D/5s is located under an isolation cover to minimize influences on the seismometer mechanics due to varying temperatures. Right: Hyposensor installed in mini-borehole at CST05
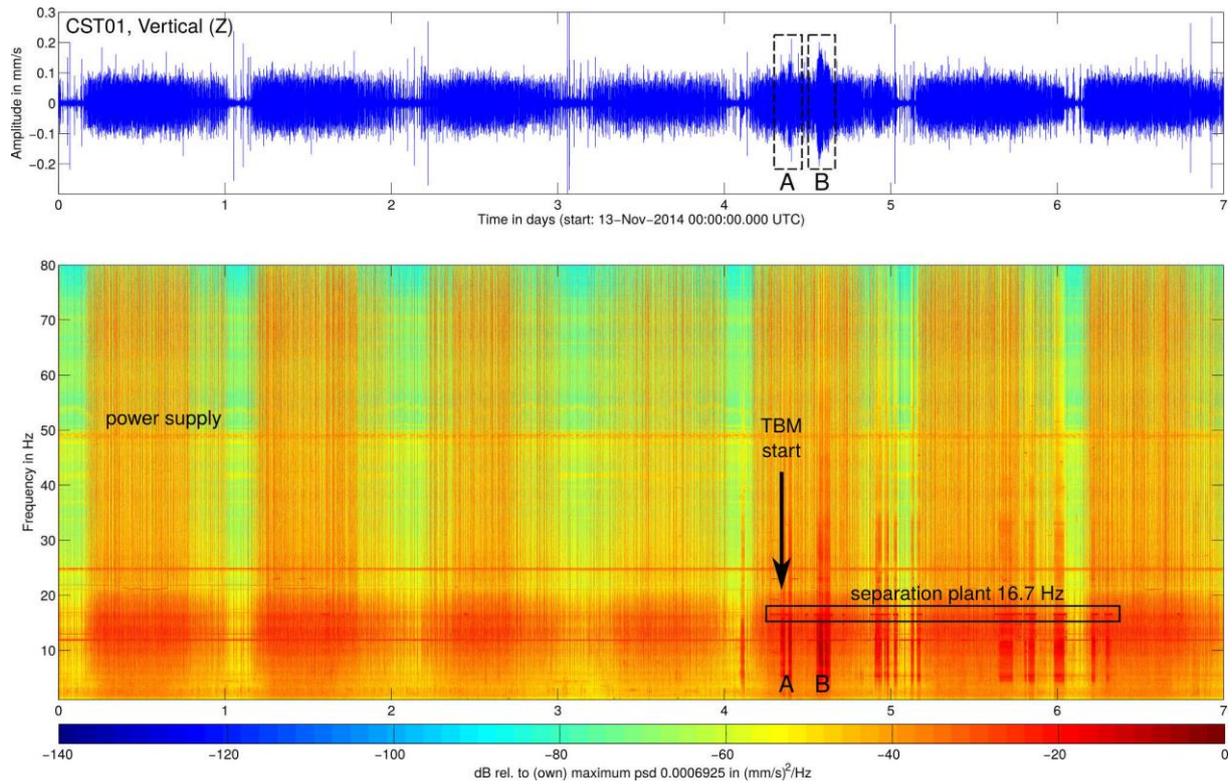
Fig. 3 One week of recorded seismic data (1-80 Hz) on the vertical component (Z) of station CST01 in the time domain (top panel) and time-frequency domain (bottom panel). The operation start of the TBM on 17/11/2014 is marked with an arrow. During time periods A and B the increased TBM signals are visible in the time domain (top panel) as well as in the time-frequency domain (bottom panel)
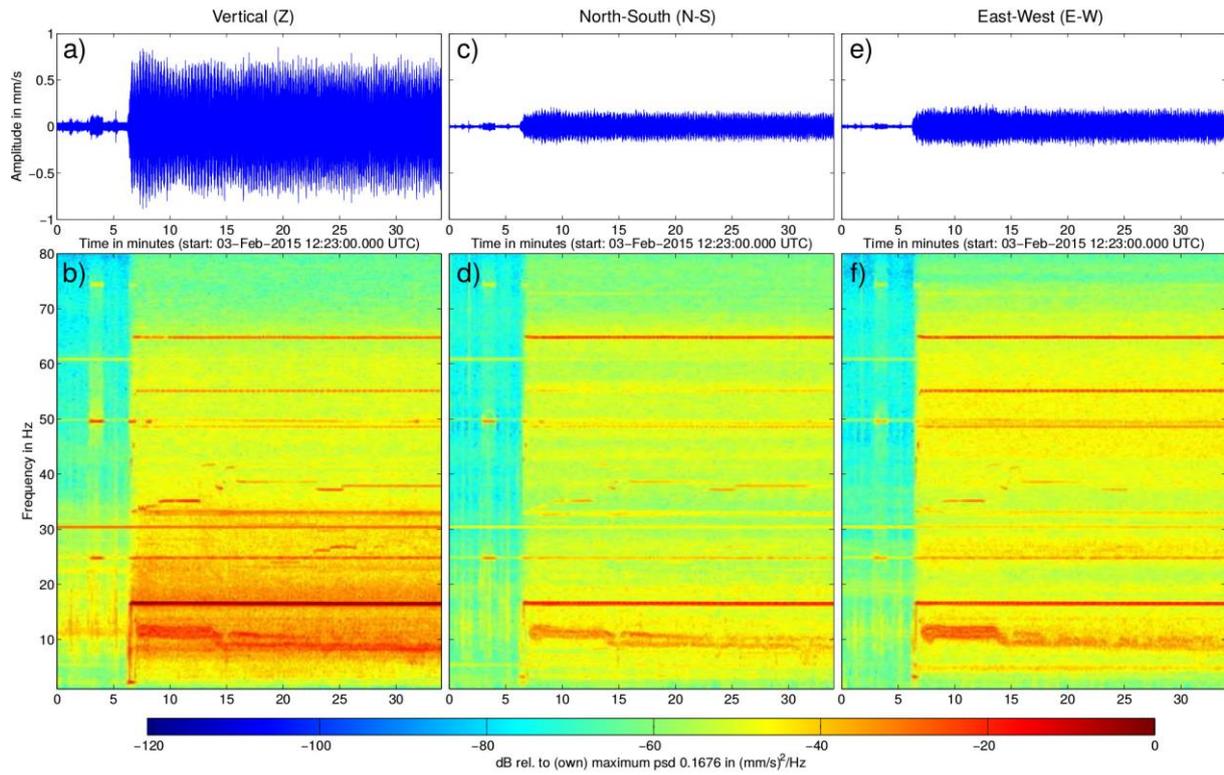
Fig. 4 *S*eismic data (1-80 Hz) recorded at the base of the separation plant in the time domain (top panels) and time-frequency domain (bottom panels) for the vertical (Z), north-south (N-S) and east-west (E-W) components. Each spectrogram is normalized to the absolute maximum out of all three spectrograms which allows a direct comparison of the spectral amplitudes
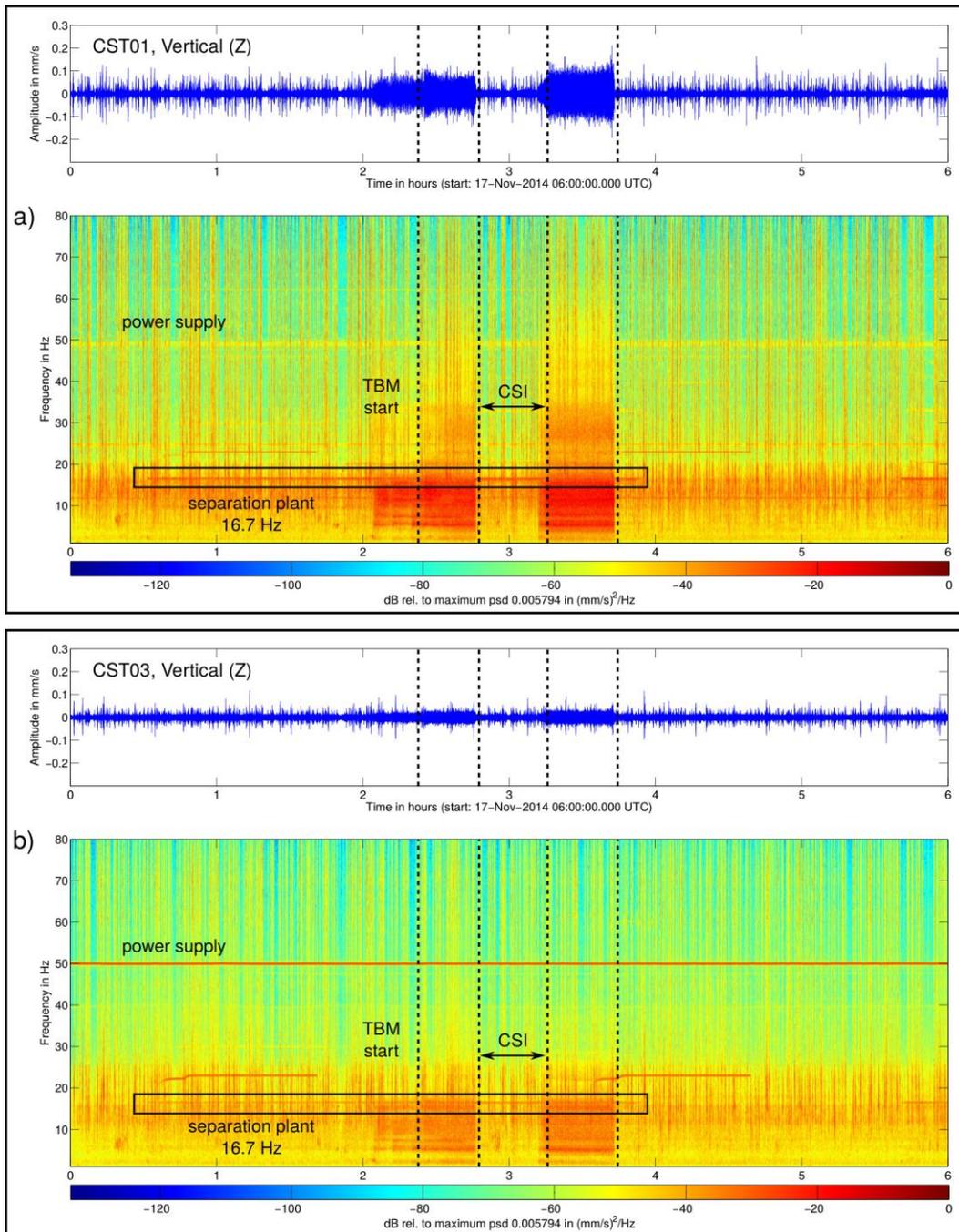
Fig. 5 Recorded seismic signals (1-80 Hz) between 06:00 and 12:00 (UTC) on 17/11/2014 in the time domain (top panels) and time-frequency domain (bottom panels) on the vertical components (Z) of stations a) CST01 and b) CST03. Each spectrogram is normalized to the absolute maximum out of both which allows a direct comparison of the spectral amplitudes. Vertical dashed black lines mark start and stop times of TBM drilling provided by the operator. The arrow indicates a concrete segment installation (CSI) period between two drilling cycles
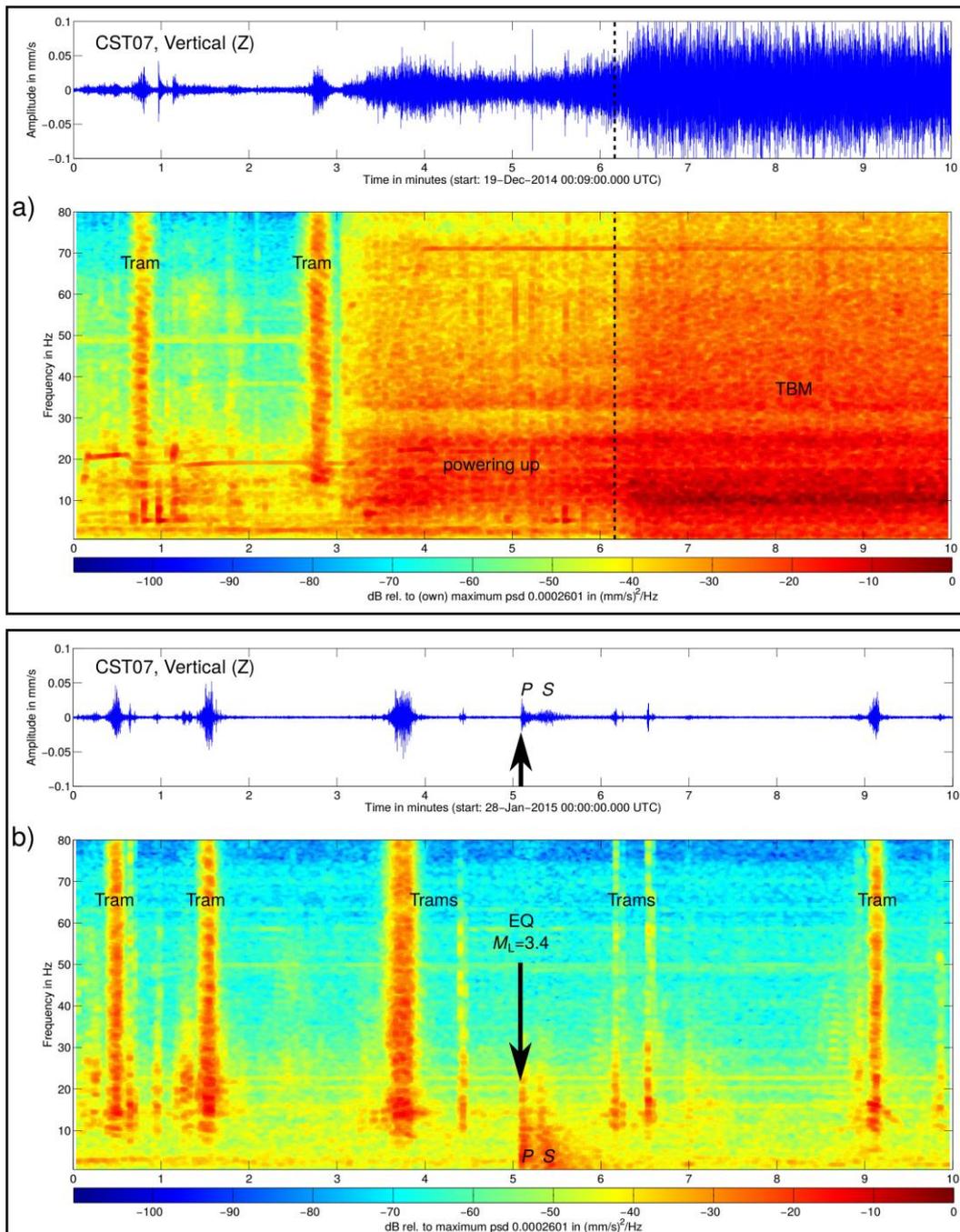
Fig. 6 Recorded seismic signals (0.6-80 Hz) on the vertical component (Z) of station CST07: a) Ten minutes on 19/12/2014 in the time domain (top panel) and time-frequency domain (bottom panel). b) Ten minutes on 28/01/2015 in the time domain (top panel) and time-frequency domain (bottom panel). Each spectrogram is normalized to the absolute maximum out of both which allows a direct comparison of the spectral amplitudes
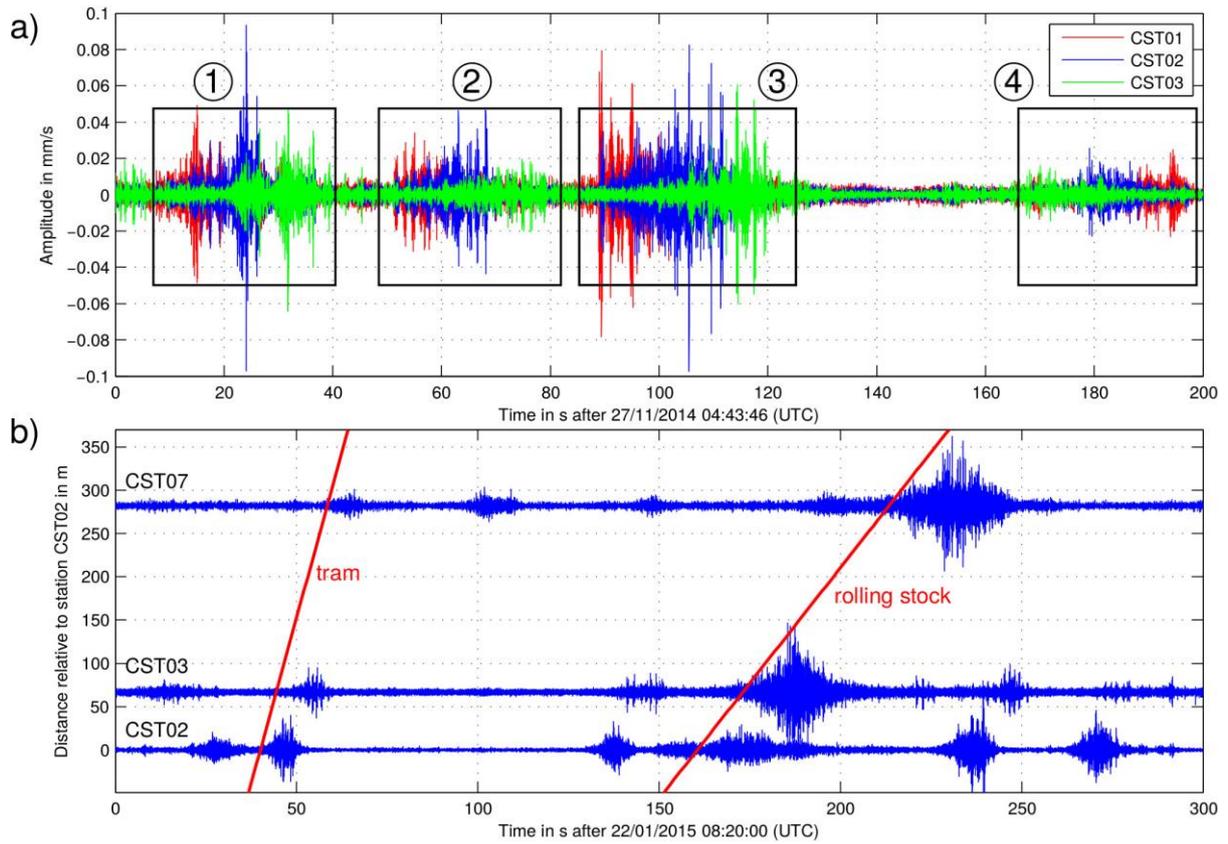
Fig. 7 a) Overlayed time series of identical time periods on the vertical components (Z) of recording stations CST01-03 (red, blue and green time series). b) Amplitude-normalized time series within identical time periods on the vertical components of recording stations CST02, 03 and 07 versus the distance relative to recording station CST02
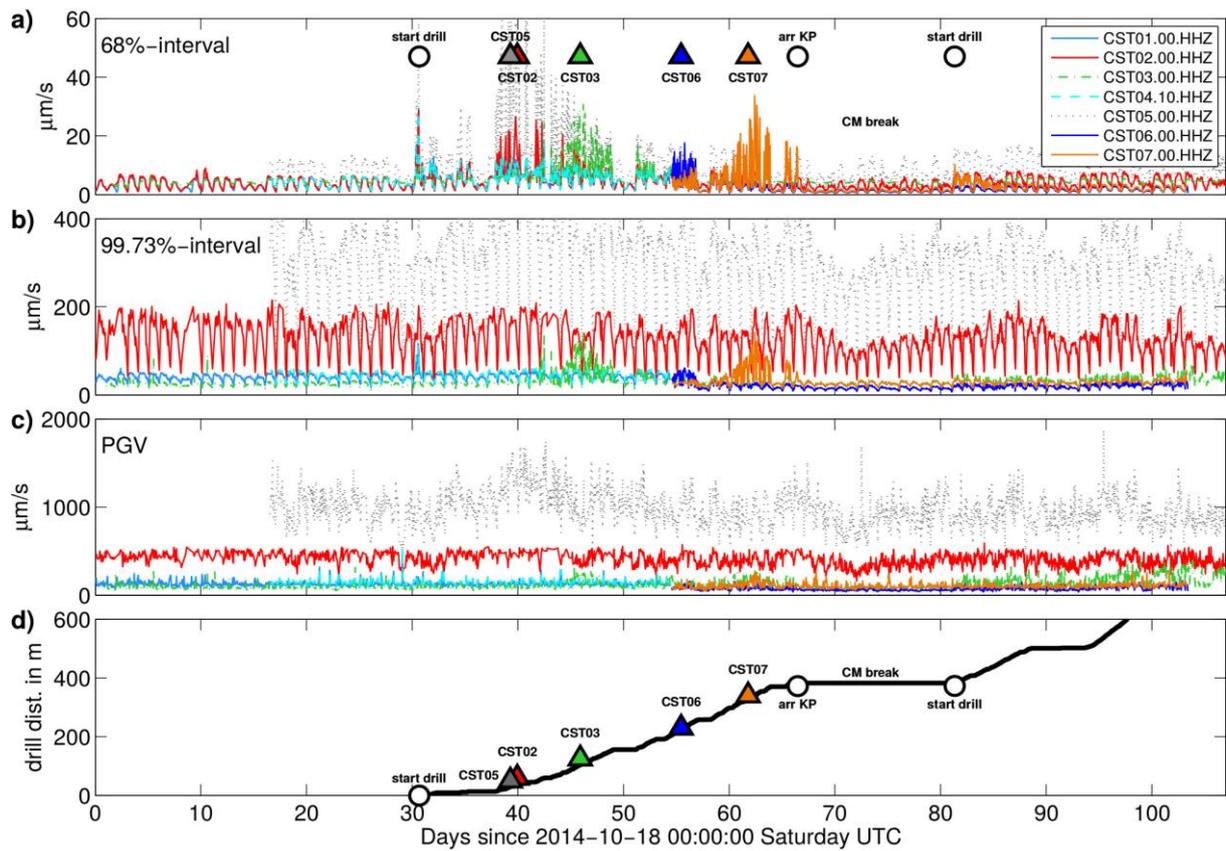
Fig. 8 a) - c) Seismic noise conditions in three different occurrence intervals and d) covered distance of the TBM versus time. Times when the TBM passes the different stations (except CST01 and CST04) are marked with triangles in the top and bottom panels. Important time stamps are the drill start, arrival at the Kronenplatz (arr KP, see Fig. 1), the following Christmas break (CM break) and continuation of drilling on 07/01/2015
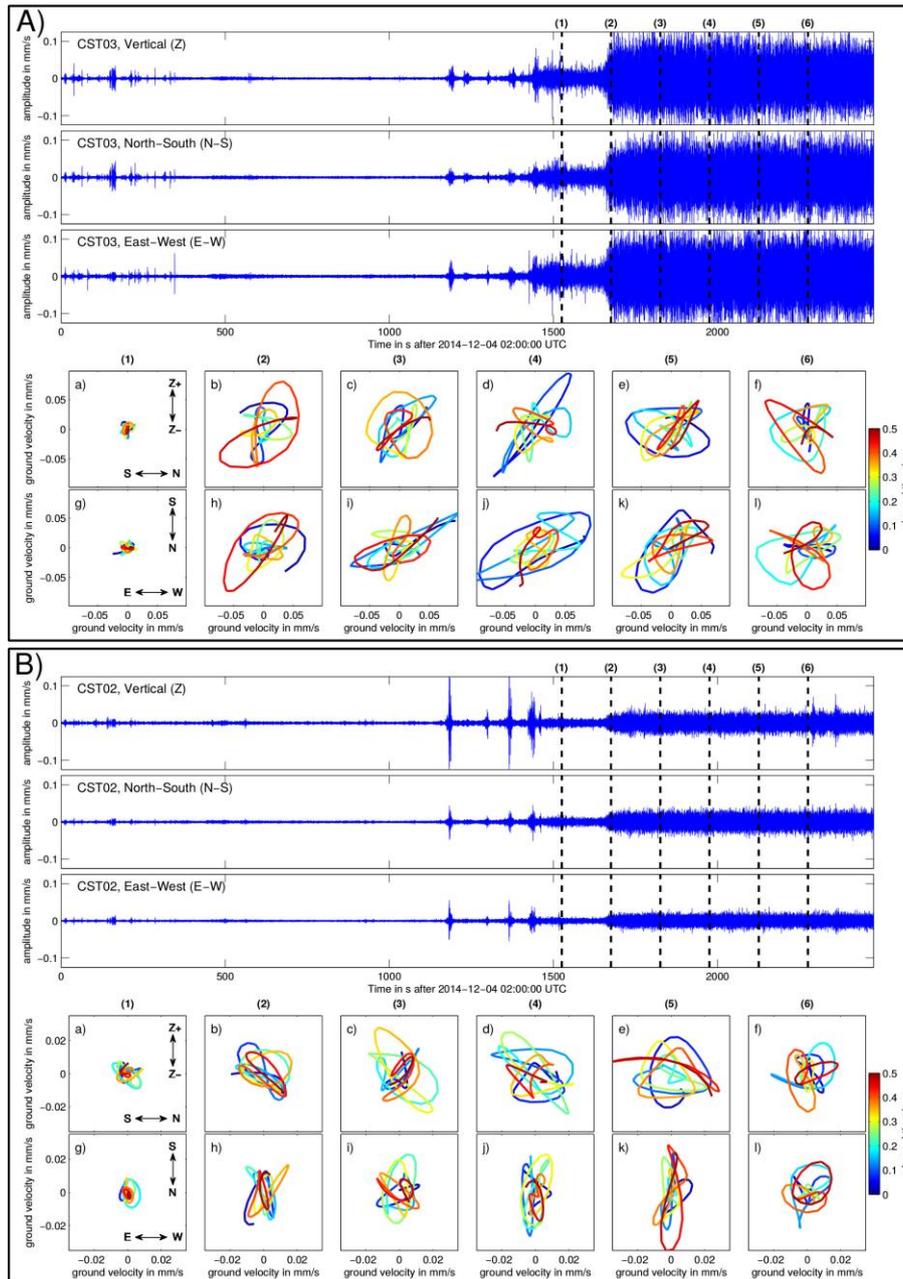
Fig. 9 Waveforms and particle motion diagrams during the operation of the tunnel boring machine. A) Recordings of station CST03 at just 10-20 m distance from the source. The particle motion diagrams contain 0.5 s of the recorded ground velocity (time windows 1-6) in the vertical vs. N-S (a-f) and N-S vs. E-W (g-l) directions. The elapsed time is indicated in colour. B) Recordings of station CST02 at 70 m distance with their corresponding particle motion diagrams
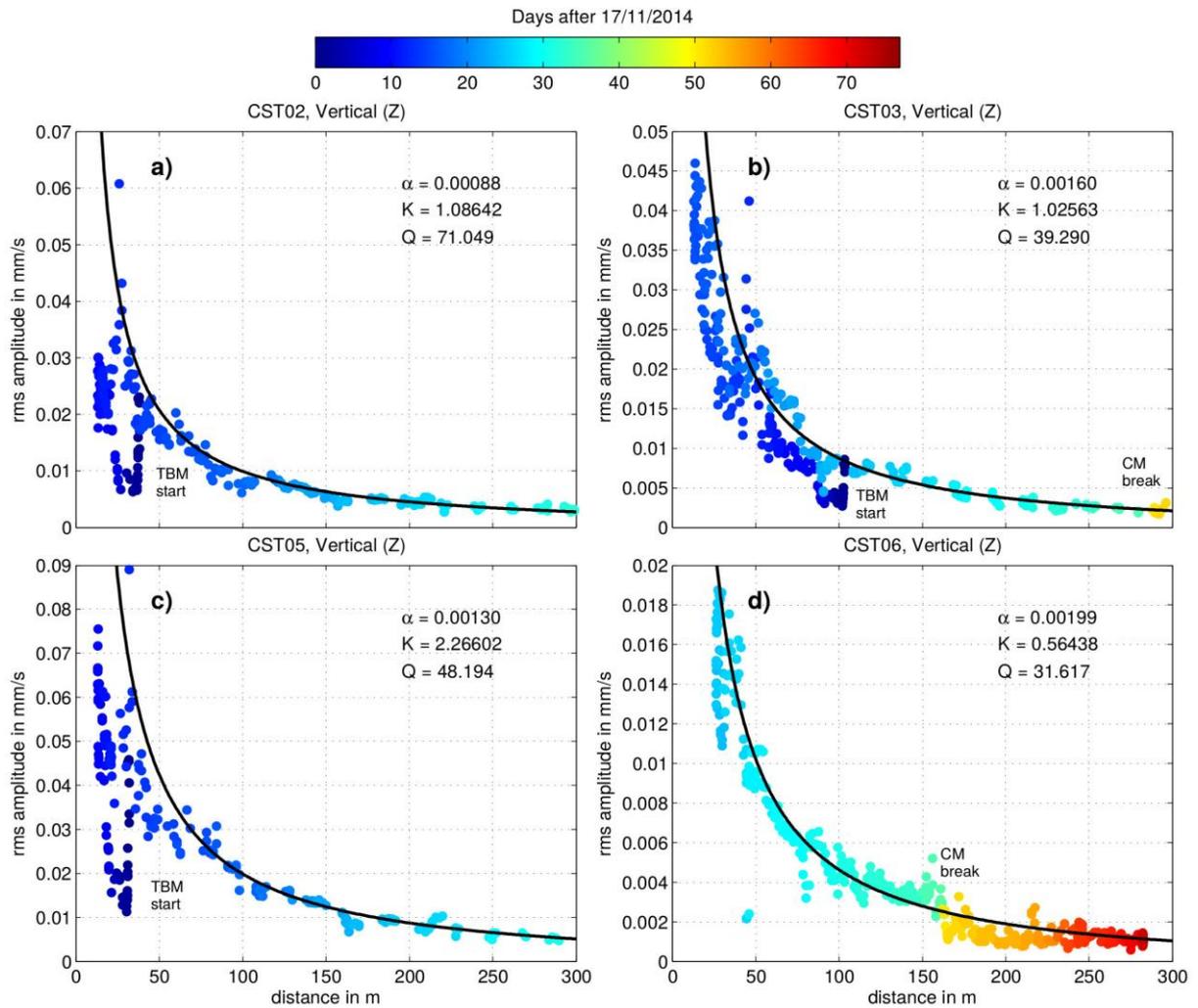
Fig. 10 a) - d) Relation between ground motion velocity (rms) and distance from the TBM (attenuation relation) for the vertical components (Z) of the four recording stations CST02, 03, 05 and 06. The temporal distributions of the estimated rms values are color coded for each station. The rms amplitudes generated due to the initial operation of the TBM on 17/11/2014 are marked in a)-c). Additionally, in b) and d) the Christmas break (CM break) from 23/11/2014 until 07/01/2015 is marked
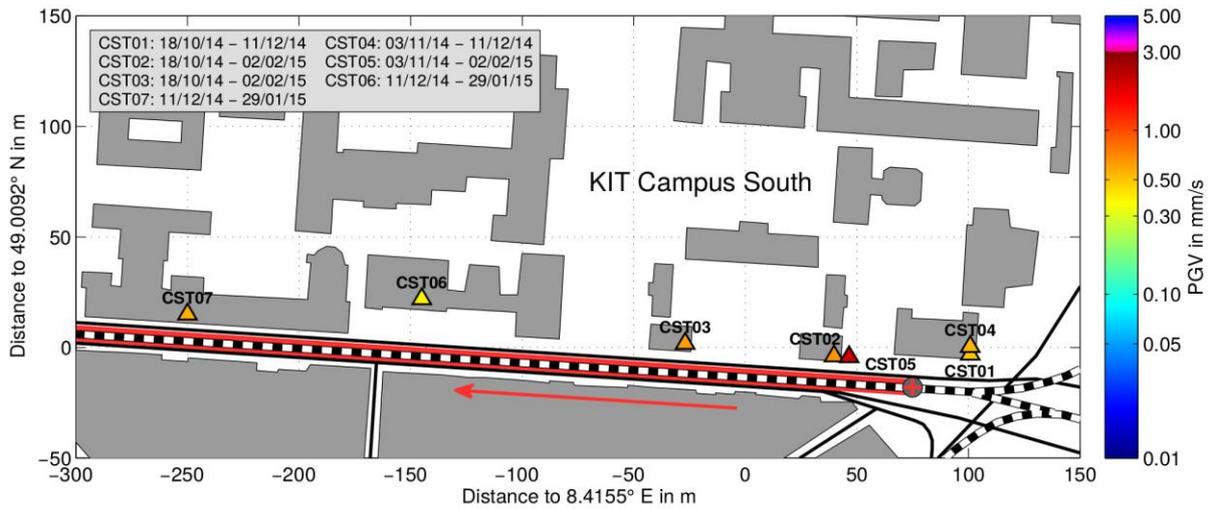
Fig. 11 PGV values determined at the different recording stations within the time periods given in the gray box in the upper left corner. The drilling route and direction are displayed in red, the drilling start position is marked as red cross (for wider area see Fig. 1). Gray areas indicate buildings and black lines roads. Rails for trams are marked as dashed lines (black and white). The limits of 3 mm/s and 5 mm/s are not reached at any station during the recording period (pink to purple colors in the colorbar)

Table 1 Determined PGV values of the single components (Z, N-S and E-W) of each station. The absolute PGV values used in Fig. 11 are marked in bold

Station	PGV_Z in mm/s	PGV_N in mm/s	PGV_E in mm/s
CST01	**0.5004**	0.3964	0.1916
CST02	**0.6555**	0.4131	0.4826
CST03	0.3995	**0.6096**	0.5759
CST04	**0.5484**	0.2127	0.1172
CST05	1.8784	**2.0844**	1.7467
CST06	**0.3911**	0.2037	0.1911
CST07	0.2799	**0.5569**	0.3168